Spectrochimica Acta Part B 63 (2008) 1151–1158

Contents lists available at ScienceDirect

Spectrochimica Acta Part B

journal homepage: www.elsevier.com/locate/sab

Evaluation of laser induced breakdown spectroscopy for the determination of macronutrients in plant materials ☆

Lilian Cristina Trevizan [a,*], Dário Santos Jr. [b], Ricardo Elgul Samad [c], Nilson Dias Vieira Jr. [c], Cassiana Seimi Nomura [d], Lidiane Cristina Nunes [e], Iolanda Aparecida Rufini [a], Francisco José Krug [a]

[a] Centro de Energia Nuclear na Agricultura, Universidade de São Paulo, Av. Centenário 303, 13416-000, Piracicaba-SP, Brazil
[b] Universidade Federal de São Paulo — UNIFESP, Rua Prof. Artur Riedel 275, 09972-270, Diadema-SP, Brazil
[c] Centro de Lasers e Aplicações, IPEN/CNEN-SP, Av. Prof. Lineu Prestes 2242, 05508-000, São Paulo-SP, Brazil
[d] Centro de Ciências Naturais e Humanas, Universidade Federal do ABC, Rua Santa Adélia 166, 09210-170, Santo André-SP, Brazil
[e] Departamento de Química, Universidade Federal de São Carlos, Rod. Washington Luís, km 235, 13565-905, São Carlos-SP, Brazil

ARTICLE INFO

Article history:
Received 30 November 2007
Accepted 13 August 2008
Available online 23 August 2008

Keywords:
LIBS
Plant analysis
Macronutrients

ABSTRACT

Laser induced breakdown spectroscopy (LIBS) has become an analytical tool for the direct analysis of a large variety of materials in order to provide qualitative and/or quantitative information. However, there is a lack of information for LIBS analysis of agricultural and environmental samples. In this work a LIBS system has been evaluated for the determination of macronutrients (P, K, Ca, Mg) in pellets of vegetal reference materials. An experimental setup was designed by using a Nd:YAG laser operating at 1064 nm and an Echelle spectrometer with ICCD detector. The plasma temperature was estimated by Boltzmann plots and instrumental parameters such as delay time, lens-to-sample distance and pulse energy were evaluated. Certified reference materials as well as reference materials were used for analytical calibrations of P, K, Ca, and Mg. Most results of the direct analysis of plant samples by LIBS were in reasonable agreement with those obtained by ICP OES after wet acid decomposition.

1. Introduction

Essential elements play a decisive role in plant nutrition and can affect crop yields when not present in appropriate concentration levels. Thus, the determination of macronutrients (N, P, K, Ca, Mg, S) and micronutrients (Fe, Cu, Mn, Zn, B, Mo, Ni and Cl) in plant materials is recommended to evaluate the nutritional status of crops of economic interest, if yields are to be maintained at a high and desirable efficient production level.

Macronutrients deficiency can cause severe problems in plant growth and appearance. Plants suffering from P deficiency are small and have a bluish green colour in the early stages of growth. In addition, fruit trees show reduced growth of new shoots and flower initiation is impaired [1]. On the other hand, potassium deficiency does not immediately result in visible symptoms, but affected plants show increased susceptibility to frost damage and fungal attack. Calcium plays a key role in plant growth and development and the deficiency can deform young leaves. Magnesium deficiency symptoms differ between plant species but an inadequate supply depresses shoot and root growth [1]. The expected range of concentrations of the macronutrients in plant leaves of crops in good nutritional status, assumed for most plants of agricultural interest, vary in the following ranges (dry matter basis): 0.8–10 g kg^{-1} P, 6–60 g kg^{-1} K, 2–60 g kg^{-1} Ca and 1–10 g kg^{-1} Mg.

Generally, essential elements determination in most routine laboratories requires sample pre-treatments such as washing, drying and grinding with further wet acid decomposition in open or closed systems. The most recommended method for large routine analysis of the acid digests is ICP OES, due to its inherent multielemental and simultaneous analytical capabilities. For instance, the macronutrients P, K, Ca, Mg, and S as well as the micronutrients Fe, Cu, Mn, Zn and B can be determined in approximately 30 s in each acid digest.

Alternatively, atomic absorption spectrometry can be successfully used for K, Ca, Mg, Fe, Cu, Mn and Zn determinations in air-C_2H_2 flame, flow injection spectrophotometry for P and B, and flow injection turbidimetry for S determination in the same acid digest. For plant diagnosis, in addition to the above mentioned analytes, it is also necessary to determine N and this task requires another digestion method.

All these methods have been used at CENA laboratory in the last 30 years for large routine scale analysis. However, there is still an analytical challenge, not fully solved, for the direct analysis of plant materials. In the past, there was an attempt in our laboratory to use

☆ This paper was presented at the Euro Mediterranean Symposium on Laser Induced Breakdown Spectroscopy (EMSLIBS 2007) held in Paris (France), 11–13 September 2007, and is published in the Special Issue of Spectrochimica Acta Part B, dedicated to that conference.

* Corresponding author. Fax: +55 19 34294610.
E-mail address: lilian@conectcor.com.br (L.C. Trevizan).

0584-8547/$ – see front matter © 2008 Elsevier B.V. All rights reserved.
doi:10.1016/j.sab.2008.08.005

dc-arc optical emission spectrometry for this purpose, by making conductive pellets just mixing high purity graphite powder with ground plant materials, but the idea was not easily implemented because of the lack of certified reference materials for calibration, difficulties for appropriated sample mixing and impossibility to determine K and S (no analytical channels available in the simultaneous atomic emission spectrometer).

In spite of the growing interest for LIBS demonstrated in the recent literature [2–5] there are very few applications dealing with the analysis of biological materials. A multi-elemental method for direct solid analysis of plant leaves by LIBS was evaluated by Sun et al. [6] for the determination of three macronutrients (Ca, Mg and P), four micronutrients (Fe, Cu, Mn, and Zn) and Al. NIST certified reference materials and mixtures of these materials in different proportions were used for calibration. The powdered leaf sample was applied directly on a double-sided tape on a glass slide and a 100 mJ/pulse Nd:YAG laser at 1064 nm was used to form the laser induced plasma. Best signal to noise was obtained after 1 μs delay time and 10 μs integration time. Six groups of 20 single shots were programmed for each of the three tapes mounted on glass slides, and laser shots on the tape did not overlap each other. The coefficient of variation of measurements made in one slide was about 8–15%. It was concluded that a fast and easy analytical method was provided for the determination of the above mentioned analytes in botanical materials, agricultural food products and materials of similar matrix. Accuracy was checked by using Spanish moss for Mn and Zn and pine needles for P, Fe, Cu and Al. There was no additional information for Ca and Mg.

In 2001, Cho et al. [7] proposed a method for determination of K and Mg in starch-based flours by a Q-switched Nd:YAG laser and a photodiode array detector. The starch powder samples or NIES standards were mixed well with 50% (w/w) cellulose to improve sample rigidity for efficient laser induced plasma formation. Limits of detection were 0.4 and 3 μg g^{-1} respectively for Mg 279.553 nm and K 766.490 nm. Calcium was also detected at 293.366, 396.817 and 422.673 nm, but analytical calibration curves and detection limits were not informed for this element.

LIBS has also been applied for analysis of the spatial resolution of nutrients and contaminants in vegetal tissues. Kaiser et al. [8] compared X-ray radiography and femtosecond LIBS for spatial resolution of Cd and Pb in leaves and roots. However, it was pointed out that quantitative results were not obtained because standard samples of leaves were not available. In another work, Samek et al. [9] used a femtosecond laser for the determination of Fe in leaf vein and parts of leaf positioned between the veins, a procedure that can show topochemical information with high spatial resolution and sensitivity.

Gornushkin et al. [10] used a Nd:YAG laser and an charged couple device (CCD) detector for Mg detection in powdered samples and investigate the influence of the matrix on the Mg signals. They suggested the use of Mg II weak lines at 292.87 and 293.65 nm that appeared only at concentrations above 0.7%. In contrast, they used the ionic lines at 279.806 and 280.27 nm and the atomic line at 285.213 nm that are extremely strong and could be seen even at very low concentrations (below 0.001%). However, these lines show strong self-absorption at concentrations above 0.5%, reducing the linear dynamic range for analysis. The surface density normalization method proposed in the work was useful for the reduction of matrix effects in the determination of Mg in powdered samples of different composition. Accuracy of the method for the determination of Mg in plant materials such as spinach, peach and apple leaves was not shown.

There is an additional contribution dealing with Ca determination in sunflower seedling [11] by using both ns and fs LIBS. The two strong lines of Ca at 393.4 and 396.8 nm were used. Water sample was used for analytical performance evaluation and detection limits were 4 and 16 mg l^{-1} Ca with nanosecond and femtosecond lasers, respectively.

In summary, in spite of the above-mentioned contributions, there is very few information for the validation of LIBS methods dealing with the determination of essential macro and micronutrients in plant materials aiming diagnosis of crops nutritional status.

The aim of this work is to show the results of the determination of macronutrients (P, K, Ca and Mg) in pellets of powdered samples by using a LIBS system designed for routine analysis. Certified reference materials and reference materials from NIST, NIES, GBW and IAEA were used for calibration and method performance was compared to ICP OES after wet digestion of plant samples.

2. Experimental setup

2.1. LIBS instrumentation

Experiments were carried out with a Q-switched Nd:YAG laser (Brilliant, Quantel, France) operating at the fundamental wavelength (1064 nm), generating 5 ns pulses of (365±3) mJ, in a 6 mm diameter beam with quality factor M^2 smaller than 2, at 10 Hz repetition rate. The laser pulses were focused on the sample pellet by a 20 cm focal length converging lens. The lens-to-sample distance was adjusted to assure a high signal-to-noise ratio and the lowest standard deviation of measurements between successive sampling spots. Individual samples were placed in a manually controlled two-axes translation stage that was moved in the plane orthogonal to the laser propagation direction. To collect the plasma emission, a telescope, composed of fused silica lenses, was assembled. Two lenses were used: a short focal distance lens (5 cm) maximized the plasma emission collection solid angle, and a longer focal length lens (12.5 cm) injected the collected light into the 600 μm core spectrometer fiber. The telescope collection angle with respect to the laser optical axis was 25 degrees.

A model ESA 3000 spectrometer (LLA Instruments GmbH, Germany) equipped with Echelle optics and focal length of 25 cm with numerical aperture of 0.22, which provides a 24.5×24.5 mm^2 flat image plane, was employed. This system is a compromise that offers maximum resolution in the wavelength range between 200 and 780 nm with resolving power ranging from 10.000 to 20.000. The linear dispersion per pixel ranges from 5 pm at 200 nm to 19 pm at 780 nm. The wavelength calibration was checked using Hg and Zn atomic lines from electrodeless discharge lamps (EDL II System, Perkin Elmer, Germany). The detector is an ICCD camera, comprised of a Kodak KAF 1001 CCD array of 1024×1024 pixels full frame (24×24 μm^2) and a microchannel plate image intensifier of 25 mm diameter coupled to a UV-enhanced photocathode. The image signals are digitalized in dynamic range of 16 bits and further processed by an industrial computer. The features of using echelle spectrometers equipped with ICCD for analysis by LIBS methods can be found elsewhere [12].

The dark current of the ICCD was automatically subtracted from the measured spectral data. For all measurements presented in this work, the integration time and the number of accumulated pulses were fixed at 5 μs and 8 pulses, respectively.

2.2. Samples and reference materials

Bean leaves were used for the estimation of plasma temperature and temporal characterization of emission lines. Leaves of 11 plant species were analyzed by the proposed LIBS system. Samples were lyophilized, ground in a knife mill model MA340 (Marconi, Brazil) and homogenized by using a cryogenic mill with a laboratory self-container liquid nitrogen bath model MA-775 (Marconi) during 2 min. The potentialities of using cryogenic grinding in other analytical applications are described elsewhere [13–15].

The following certified reference materials and reference materials were used for calibration: bush branches and leaves (National Research Centre for CRM's — GBW 07603), cabbage (International Atomic Energy Agency — IAEA 359), soya flour (IAEA 361), rice flour (National Institute for Environmental Studies — NIES 10-c), apple leaves (National Institute of Standards and Technology — NIST 1515), peach leaves (NIST 1547), wheat flour (NIST 1567a) and spinach leaves (NIST 1570a). The materials

Table 1
Fe I parameters for Boltzmann temperature determination (λ = wavelenght, *A* = transition probability, *E* = energy, *g* = statistical weight of the level)

λ (nm)	*A* (s^{-1})	*E* (eV)	*G*
267.906	$1.90 \cdot 10^7$	5.5	11
273.358	$8.60 \cdot 10^7$	5.4	9
278.810	$6.30 \cdot 10^7$	5.3	13
300.957	$1.70 \cdot 10^7$	5.0	9
330.634	$6.10 \cdot 10^7$	6.0	5
339.933	$3.80 \cdot 10^7$	5.8	5
373.713	$1.42 \cdot 10^7$	3.4	9
344.387	$6.20 \cdot 10^6$	3.7	3
347.670	$5.40 \cdot 10^6$	3.7	3
376.554	$9.80 \cdot 10^7$	6.5	15
376.720	$6.40 \cdot 10^7$	4.3	3
364.784	$2.92 \cdot 10^7$	4.3	11
365.146	$6.20 \cdot 10^7$	6.2	9
382.782	$1.05 \cdot 10^8$	4.8	5
384.105	$1.30 \cdot 10^8$	4.8	3
406.359	$6.80 \cdot 10^7$	4.6	7
407.173	$7.65 \cdot 10^7$	4.7	5

Data from reference [24].

were homogenized by using a cryogenic mill prior to the analysis. Pellets were prepared in a Spex model 3624B X-Press by transferring 0.5 g of powdered material to a 15 mm die set and applying a 8.5 ton cm^{-2} during 10 min. The pellets were approximately 3 mm thick and 15 mm diameter. At least ten spectra were collected in different test portions of the sample pellet.

For comparative purposes, plant samples and NIST certified reference materials were also digested with nitric and perchloric acids using a block digestor (Marconi, Piracicaba, Brazil). Samples were decomposed in triplicate according to the following procedure: 500 mg of dried and ground material was kept overnight (ca 12 h) with 5.0 ml of 14 mol l^{-1} HNO_3 at room temperature in a fume hood. Then, the mixture was pre-digested at a temperature not exceeding 160 °C (ca 3 h). After cooling, the excess of nitric acid was driven off by adding 1.3 ml concentrated $HClO_4$ and increasing the block digestor temperature to 210 °C. Heating was continued until a clear colorless solution was obtained and dense fumes of perchloric acid dihydrate appears. After cooling the digests were diluted with water up to 50 ml and analysed by ICP OES (Vista RX, Varian, Australia).

3. Results

3.1. Experimental conditions

Plasma temperature can be estimated using the Boltzmann plot from relative line intensities, if their transition probabilities (A) from a given excited state are known [2,5,16–18]. In order to improve temperature values, many lines should be used simultaneously and a graphic is produced as result of Equation 1:

$$\ln(I\lambda/gA) = -E/kT - \ln(4\pi Z/hcN_o) \quad (1)$$

where *I* is the line intensity, λ is the line wavelength, *g* is the statistical weight of the level, *E* is the energy of the upper state, *k* is the Boltzmann constant, *T* is the temperature, *Z* is the partition function usually taken as the statistical weight of the ground state, *h* is the Plank constant, *c* is the speed of light and N_o is the population of the ground state.

The graph of the right term of Eq. (1) as a function of E results in a straight line with slope $-1/kT$. In this work, temperature was estimated by using atomic Fe lines emitted from the microplasma formed in the sample pellet of bean leaves. The spectroscopic constants used for the Boltzmann plots are summarized in Table 1. Line intensity measurements were taken with the accumulation of 8 pulses and the estimated temperature corresponded to (9130 ± 130) K by using 2 μs delay time (Fig. 1). This result is in agreement with the literature [2] that reports values typically in the range 8000–12,000 K at 1–2 μs delay time and with an irradiance of approximately 10^{10} W cm^{-2}. Just for information, the estimated temperatures were (9410 ± 120) K with 1 μs and (8800 ± 290) K with 4 μs delay times.

By making 10 measurements in different positions of the sample pellet the coefficients of variation of the calculated temperatures were lower than 3.5%. It should be mentioned that the method is accompanied by systematic errors related to uncertainties on the transition

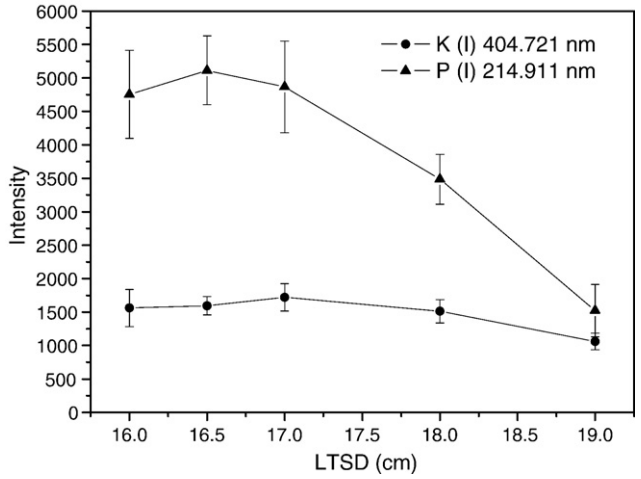

Fig. 2. Net intensities of K I and P I in function of lens-to-sample distance (LTSD).

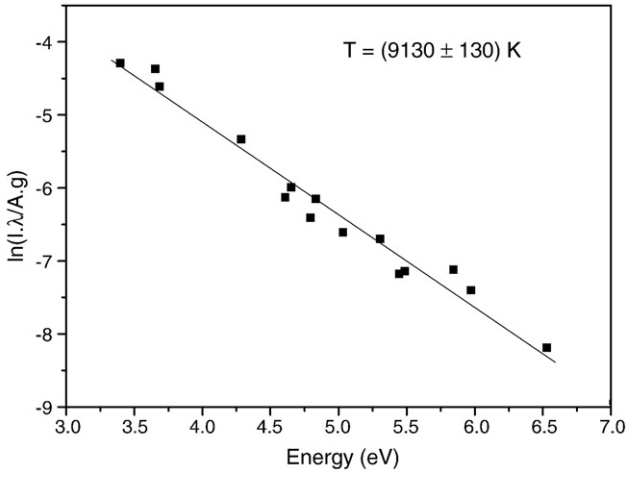

Fig. 1. Boltzmann plots for Fe I lines in bean leaves pellet with 2 μs of delay time.

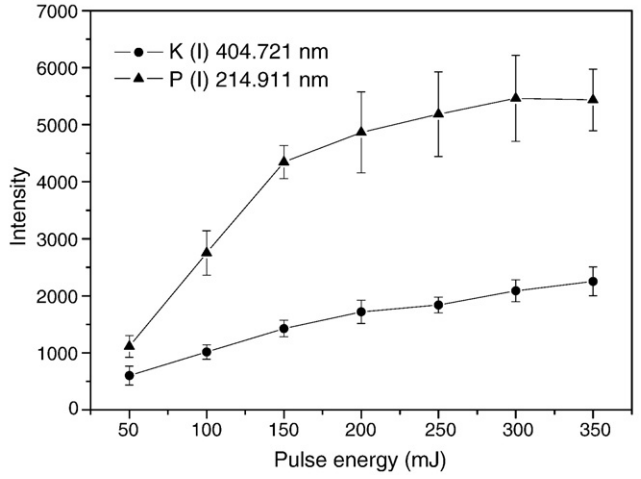

Fig. 3. Net intensities of K I and P I in function of pulse energy (LTSD: 16.5 cm).

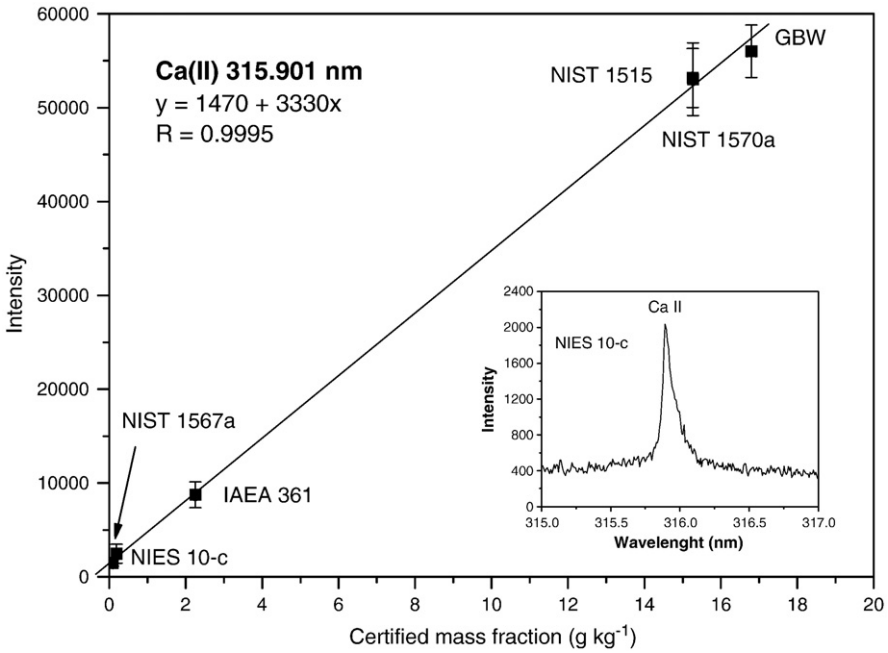

Fig. 4. Analytical calibration curve for Ca II 315.901 nm emission line using reference materials: NIES 10-c (0.095 ± 0.002 g kg^{-1}), NIST 1567a (0.191 ± 0.004 g kg^{-1}), IAEA 361 (2.25 ± 0.34 g kg^{-1}), NIST 1515 (15.26 ± 0.15 g kg^{-1}), NIST 1570a (15.27 ± 0.41 g kg^{-1}), GBW 07603 (16.8 ± 1.1 g kg^{-1}).

probabilities (A) that can reach 50% and was not considered in this work. Le Drogoff et al. [18] estimated an excitation temperature relative error of a femtosecond laser induced plasma of 20% by using atomic iron lines and Boltzmann plots.

An intense contribution of the continuum to the emission was observed when 1 μs delay time was employed. The background emission decreased continuously when higher delay times were used, and the signal-to-background ratios (SBR) did also decrease at the selected wavelengths. As a compromise in order to provide high SBR, lines discrimination and less contribution from the continuum, 2 μs delay time was chosen. Further measurements were obtained by using the same delay time. The integration time was chosen at 5 μs due to the better signal-to-noise ratio at this condition.

A detailed study was made to investigate the line intensities of laser-produced plasmas with the laser pulse energy and the lens-to-sample distance (LTSD). Take into account the inhomogeneous character of powdered samples we tried to use a higher spot area to improve signal repeatability. The laser irradiance on the sample surface depends on the LTSD and affects the emission line intensities and the mass of ablated test portion [2]. Maintaining the LTSD shorter than the lens focal length,

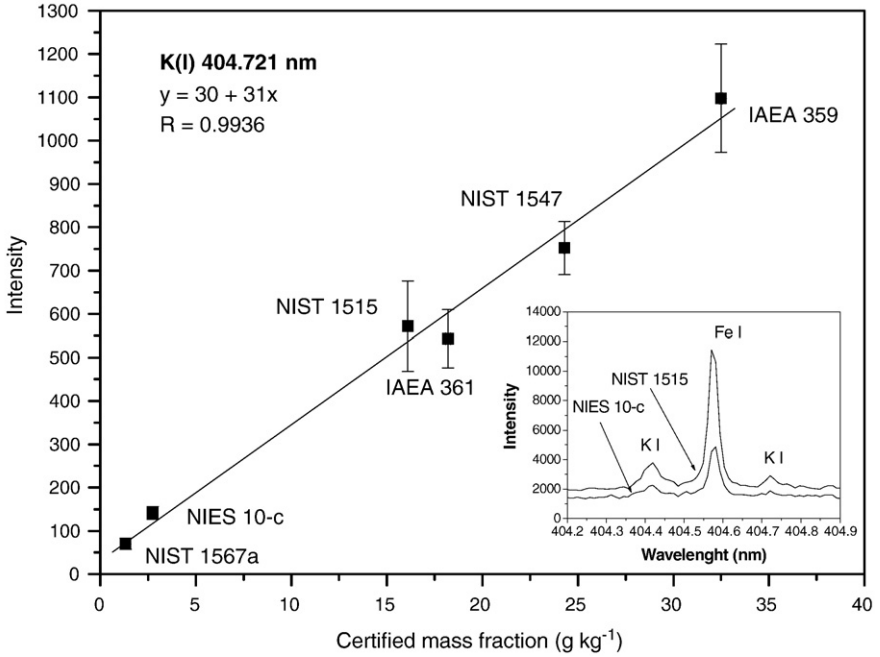

Fig. 5. Analytical calibration curve for K I 404.721 nm emission line using reference materials: NIST 1567a (1.33 ± 0.03 g kg^{-1}), NIES 10-c (2.75 ± 0.10 g kg^{-1}), NIST 1515 (16.1 ± 0.2 g kg^{-1}), IAEA 361 (18.21 ± 1.37 g kg^{-1}), NIST 1547 (24.3 ± 0.3 g kg^{-1}) and IAEA 359 (32.50 ± 0.69 g kg^{-1}).

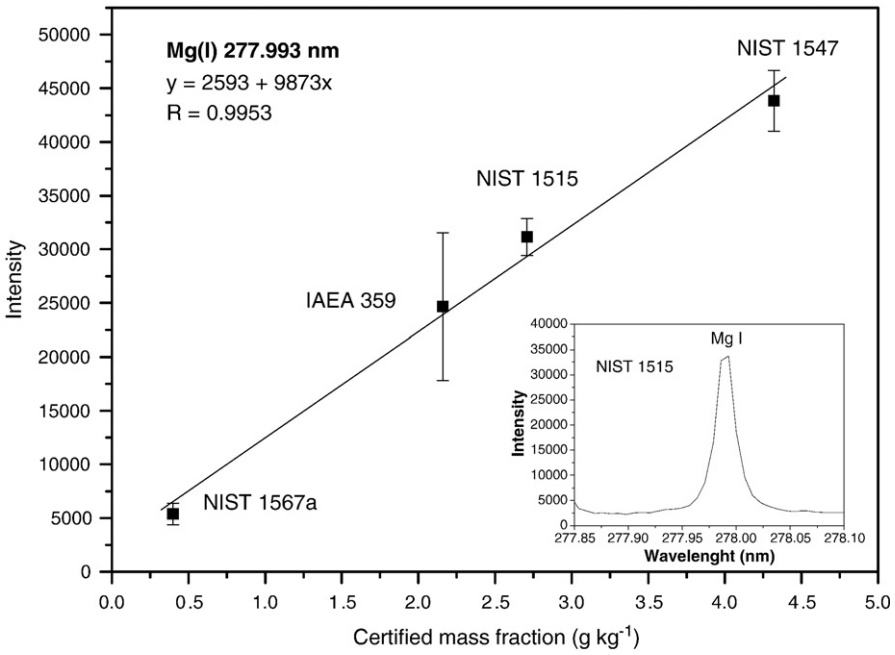

Fig. 6. Analytical calibration curve for Mg I 277.993 nm emission line using reference materials: NIST 1567a (0.40±0.02 g kg^{-1}), IAEA 359 (2.16±0.05 g kg^{-1}), NIST 1515 (2.71±0.08 g kg^{-1}), NIST 1547 (4.32±0.08 g kg^{-1}).

most of the laser energy is deposited into the material bulk [17]. We have investigated LTSD from 16 up to 19 cm in order to avoid plasma shielding effect nearby the laser beam waist at high energies. As expected, best repeatability was obtained at those conditions where shielding was minimized and line intensities were higher. Results for K (I) at 404.721 nm and P (I) at 214.911 nm indicated that there was no significant differences in the emission signals from 16 to 17 cm (Fig. 2), and the LTSD was kept at 16.5 cm in further experiments. At distances higher than 17 cm there was a decrease in line intensities probably due to the plasma shielding effect. Similar results were obtained for Ca and Mg. The optical arrangement provided a calculated beam radius of approximately 525 μm at the sample surface, resulting in a fluence and irradiance of 41.4 J cm^{-2} and 8.3 10^9 W cm^{-2}, respectively, at the maximum pulse energy (360 mJ). Under these conditions, craters of about 1.0 mm diameter were observed in the pellets.

The pulse laser energy is another instrumental parameter that affects the ablated mass test portion from the target [19]. In general, up to a certain limit, the higher the irradiance the higher the ablated mass and, consequently, the emission intensities at appropriated wavelengths increase. Emission intensities of K I at 404.721 nm and P I at 214.911 nm were monitored with pulse laser energies from 50 to 350 mJ. A significant increase in the emission signals (Fig. 3) was obtained up to 200 mJ at the LTSD chosen (16.5 cm), but no significant improvements at higher laser energies were observed. Similar results were obtained for Ca and Mg. Fluence and irradiance for 200 mJ correspond to 23 J cm^{-2} and 4.6 W cm^{-2}, respectively.

The effect of the ablation atmosphere was evaluated with argon flowing at 500 ml min^{-1} and with air. The ionic lines of Ca and Mg in the LIBS spectrum obtained under argon atmosphere was about three-fold more intense than in the presence of air, which is in agreement with data previously reported in the literature [20,21]. According to Aguilera et al. [21] the higher emission intensities in Ar were mainly due to the higher temperature of the laser-induced plasmas generated in Ar.

3.2. Calibration with certified reference materials

Analysis of pellets of reference materials were performed by applying 8 consecutive laser shots in 10 different positions at the sample surface. Data was based on cumulative spectra by using 2 μs

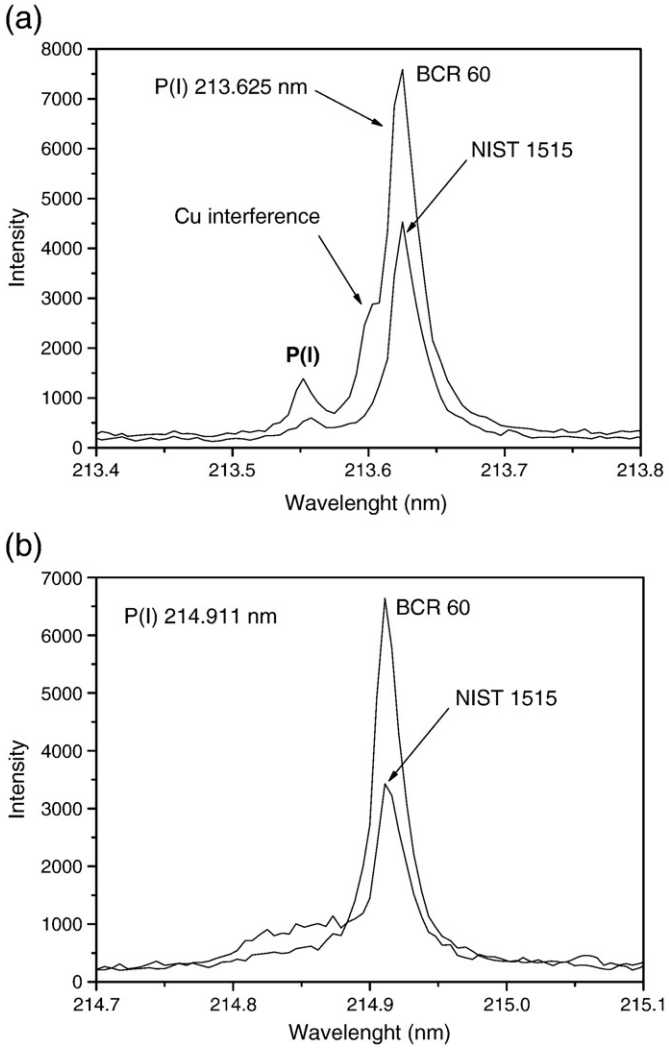

Fig. 7. Signal profile for P I lines at (a) 213.625 nm (Cu interference) and (b) 214.911 nm.

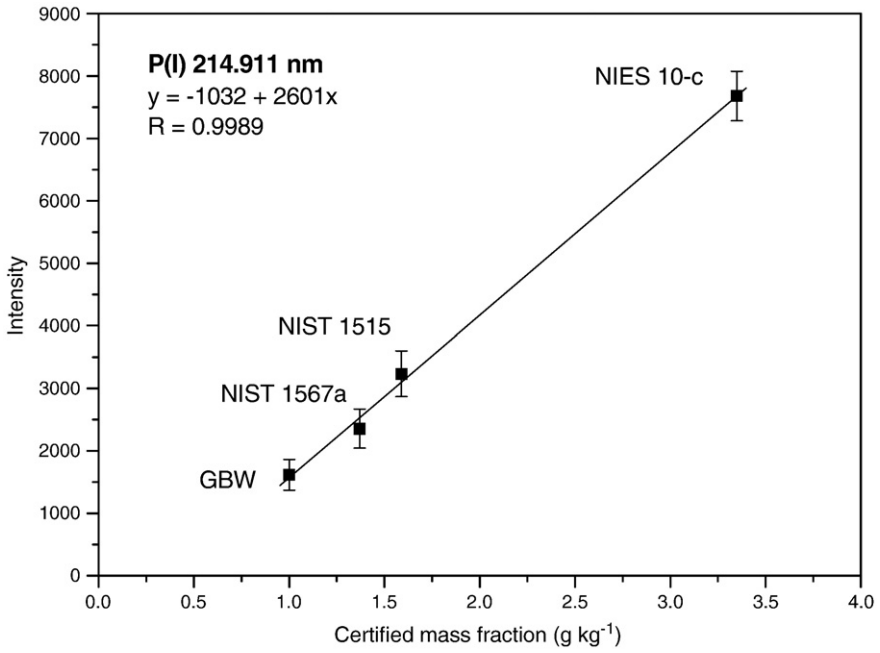

Fig. 8. Analytical calibration curve for P I 214.911 nm emission line using reference materials: GBW 07603 (1.00±0.04 g kg^{-1}), NIST 1567a (1.34±0.06 g kg^{-1}), NIST 1515 (1.59±0.11 g kg^{-1}) and NIES 10-c (3.35±0.08 g kg^{-1}).

delay time and 5 μs integration time. The LTSD was kept at 16.5 cm. For analytical calibration, most data refers to certified mass fractions. In some cases, reference materials were also used. At least results from four different materials were used in calibration curves. Although most certified values are based on a minimum sample mass of 150 mg, it was decided to see if those CRMs and RMs could fit for the calibration purpose, even knowing that the mass of the ablated test portion was much lower. By measuring the pellet mass before analysis and after laser pulses, it was observed that the ablated test portions for each 8 pulses were approximately 360 μg.

Analytical calibration curves of Ca, K and Mg are shown in Figs. 4–6, respectively. A peak profile for each wavelength used is also presented. The net emission at the defined wavelengths and certified reference materials were obtained by subtracting the background from the peak intensity of the line. Indeed, a difference in background emission was observed among the analyzed standards and samples, which was corrected by subtraction. The calculated coefficients of variation of line intensity measurements for each standard varied from 5 to 25% (n=10). According to Castle et al. [22], the estimated measurement uncertainties (Y-values) due to the laser source are lower than 4%, and one can assume that the main source of variation on data presented in this work can be attributed to analytes micro-heterogeneity in pellets, even after cryogenic grinding.

Data presented in analytical calibration curves did not include combined measurement uncertainty (Y-values) for linear correlation. According to Wunderli [23], an uncertainty term for sampling cannot be included because sampling is a different operation from measuring. If samples are taken from a homogeneous material, all measurement results for the analyte content lie within the combined measurement uncertainty and a measurement result for any individual sample within the stated probability. If not, the variations seen in the results originate from sources other than the measurement alone. The other argument stressed by Wunderli [23], is that if the analyte is distributed heterogeneously, synonymic to inhomogeneously, the results will vary much more, not because of the variability in the measurements, but because one have analyzed different samples which carry a different analyte content originating from different locations in the material batch under study. In the present work, each crater represents a different test portion, and the variation of LIBS results between test portions (n=10) represent the variation caused by the spatial distribution of the analyte content in the sample surface, i.e. most variations are due to analyte micro-heterogeneity.

Emission signals for P were detected at 213.625, 214.911, 253.571 and 255.336 nm. However, according to both NIST Atomic Spectra and Esawin software (LLA Instruments GmbH, Germany), databases, the last two lines can be interfered by Fe and Mn, respectively. The 213.625 nm line can be interfered by the Cu II 213.598 nm line. Fig. 7a presents a comparison between the P emission signal at 213.625 nm from NIST 1515 Apple leaves pellet, which contains 5.64 mg kg^{-1} Cu

Table 2
Comparison of LIBS and ICP OES results for plant analysis

Sample	Ca (g kg^{-1})		K (g kg^{-1})		Mg (g kg^{-1})		P (g kg^{-1})	
	LIBS	ICP OES	LIBS	ICP OES	LIBS	ICP OES	LIBS	ICP OES
Brachiaria leaves (*Brachiaria decumbens*)	7.65±1.83	8.76±0.03	21.62±2.97	20.47±0.21	2.24±0.47	2.54±0.01	2.17±0.56	3.20±0.04
Banana leaves (*Musa Paradisíaca sapientum*)	9.22±2.43	7.13±0.01	8.42±0.95	9.26±1.22	3.10±0.80	3.64±0.01	1.27±0.34	1.36±0.02
Coffee leaves (*Coffea arabica*)	11.69±0.96	14.44±0.07	3.46±0.30	5.69±0.10	1.90±0.17	2.14±0.02	0.62±0.08	0.56±0.01
Jack leaves (*Artocarpus integrifolia*)	12.56±1.31	10.93±0.06	13.59±2.37	13.09±0.57	1.36±0.16	2.32±0.01	0.98±0.13	1.33±0.03
Maize leaves (*Zea mays*)	13.34±0.72	17.37±0.08	28.61±3.25	22.78±0.61	5.00±0.36	5.45±0.04	1.31±0.17	1.49±0.04
Pepper leaves (*Piper nigrum*)	14.51±1.00	13.94±0.04	12.32±1.61	11.11±0.13	3.59±0.56	3.30±0.01	1.45±0.19	1.76±0.02
Soya leaves (*Glycine max*)	14.94±0.51	15.09±0.01	2.81±0.37	8.23±0.04	3.90±0.54	4.95±0.02	1.19±0.30	1.61±0.03
Guayava leaves (*Psidium guaiava*)	15.11±0.60	12.47±0.10	10.63±1.77	12.22±0.16	1.81±0.14	1.83±0.01	1.26±0.14	1.24±0.03

Uncertainties of the results are represented by one estimated standard deviation. LIBS data refers to the average results from the analysis of 10 test portions in 1 pellet (8 shots per test portion, 10 different positions); ICP OES results refers to average results of 3 measurements in each replicate of 3 digests.

and 1590 mg kg^{-1} P (uncertainties neglected) an in BCR 60 Aquatic plant pellet which contains 51.2 mg kg^{-1} Cu and 5150 mg kg^{-1} P (noncertified concentration). The P I 213.625 nm line from BCR 60 is clearly overlapped by the Cu II line. However, emission line at 214.991 nm (Fig. 7b) seems to be free from interference and was selected for analytical calibration (Fig. 8).

3.3. LIBS analysis of plant samples

Eight plant tissues, commonly found in Brazil, were analysed by the proposed LIBS system by using certified reference materials for calibration. For comparison, samples were also analysed by ICP OES after acid decomposition. Table 2 shows the results from both techniques. It should be stressed that the quality of data by ICP OES measurements was checked against the analysis of the following CRMs: NIST 1515, NIST 1567a, NIST 1570a and NIST 1547.

In general, LIBS results are in reasonable agreement with ICP OES results, but LIBS method for plant analysis must still be properly validated for each element and for each plant specie. It is necessary to make an evaluation of robustness, taking into account the effect of pellet preparation, including particle size distribution, pellet porosity, effect of binders, as well as effects of concomitants, for example. As a first set of experimental results, data can be considered a good indication that analysis of some plant materials can be carried out, but accuracy must be improved as well as the precision. In this sense, it is clear that the uncertainties associated to the LIBS results were much greater, but, again, it is assumed that the high uncertainties of LIBS results are mainly due the small test portions sampled in each pellet. As it was already mentioned, the ablated test portion for each 8 pulses was estimated to be approximately 360 μg, which is much less than the digested 500 mg test portions used in the validated method for the determinations by ICP OES. Our basic question is whether it is appropriate to compare the coefficient of variations of 10 test portions of 360 μg with 3 test portions of 500 mg and, in principle, the key point for improving the quality of LIBS results is to find what is the most appropriated test portion mass in each sample pellet. We'll get to this question in due course as additional investigations must be carry out through optimization designs to properly solve this problem. On the other hand, particularly for K, discrepant results were observed in lower concentrations and the causes for this effect is also under investigation.

The macronutrients detection limits were estimated from certified reference materials with the lowest mass fraction of each analyte in the calibration curve. As blank samples were not available, the estimated standard deviation of the background (s), measured in the surroundings of the selected emission line, was used ($n=10$) and detection limits were calculated as 3 s/b, where b is the angular coefficient of the calibration curve. The detection limits of alternative lines, that can also be used for determination of macronutrients in plant material, are presented in Table 3. Indeed, even more alternative lines can be used, depending on the analytical purpose. Particularly in the case of Mg, the ionic lines at 279.553 and 280.270 nm are the most sensitive, but these lines were saturated due to the high concentration of Mg in the ablated test portions. In order to avoid the strong self-absorption of Mg II 280.271 and Mg I 285.212 nm at concentrations above 0.5% m/m, Gornushkin et al. [10] suggested the use of Mg II weak lines at 292.863 and 293.651 nm. These lines are appropriate for plant materials with higher concentrations with estimated detection limits of 0.15 and 0.25 g kg^{-1} Mg, respectively. In general, the Mg content in plant materials (dry matter basis) varies from 1 to 10 g kg^{-1}. Except for K, the detection limits are appropriate taking into account the range of concentrations of the studied macronutrients. Strategies for improving the detection limit of K are necessary, such as the accumulation of a larger number of pulses.

Table 3
Estimated LIBS detection limits for Ca, K, Mg and P at different emission lines

Element*	Wavelength (nm)	LOD (g kg^{-1})
Ca II	315.901	0.03
Ca I	422.677	0.01
K I	404.721	3.2
K I	404.420	2.5
Mg I	280.224	0.02
Mg I	277.993	0.06
P I	214.911	0.08
P I	255.329	0.3

*I = atomic, II = ionic.

4. Conclusions

Certified reference materials can be used for the preparation of pressed pellets in order to obtain LIBS univariate calibration curves for the determination of macronutrients in plant samples using nanosecond pulses from a Nd:YAG laser at 1064 nm. Reasonable agreement with ICP OES results for plant materials was obtained, and other strategies are under investigation for the method validation, including robustness. The main difficulty for univariate calibration is that the certified values are based on sample masses of at least 150 mg, which is much higher than the ablated test portion. As the test portion is quite small, it is possible to note that the analyte is distributed heterogeneously in the sample pellet. The coefficients of variation of the results ($n=10$) varied from 5 to 25% depending on the analyte and on the reference material.

The proposed procedure is simple and fast. Sample must be only transformed in a pellet, which is done in 2 min after grinding, and the pellet is easily adapted in a compact ablation chamber. Analysis are made in each test portion in 1 s, and the number of test portions depends on sample micro-heterogeneity and lens-to-sample distance arrangement. In principle, although 10 test portions of approximately 360 μg per pellet were chosen per analysis, an increase in the number of test portions and/or in the number of shots per test portion certainly will lower the variance due to analyte inhomogeneity in the pellet. In addition, each test portion can be represented by many craters, which will result in a much higher test portion mass.

It is clear that an effort must be done for the development of more appropriate certified reference materials for better calibration towards direct microanalysis of pellets of plant materials, but we would like to address that other strategies for calibration are in course in our laboratory. In addition, data for micronutrients (Fe, Cu, Mn, Zn and B) as well as non-essential elements (Al, Si, Na) are under evaluation and will be presented in the near future.

Acknowledgment

Authors are thankful to Fundação de Amparo à Pesquisa do Estado de São Paulo (FAPESP, Processes: 04/15965-2, 06/06466-8, 05/50773-0) and to Conselho Nacional de Desenvolvimento Científico e Tecnológico (CNPq, Processes: 477385/2006-0, 301285/2006-3) for financial support.

References

[1] K. Mengel, E.A. Kirkby, Principles of Plant Nutrition, 5th ed, Kluwer Academic, Netherlands, 2001.
[2] D.A. Cremers, L.J. Radziemski, Handbook of Laser-induced Breakdown Spectroscopy, John Wiley & Sons Ltda, Chichester, 2006.
[3] A.W. Miziolek, V. Palleschi, I. Schechter, Laser-Induced Breakdown Spectroscopy, Cambridge University Press, Cambridge, 2006.
[4] J.D. Winefordner, I.B. Gornushkin, T. Correll, E. Gibb, B.W. Smith, N. Omenetto, Comparing several atomic spectrometric methods to the super stars: special emphasis on laser induced breakdown spectrometry, LIBS, a future super star, J. Anal. At. Spectrom. 19 (2004) 1061–1083.
[5] C. Pasquini, J. Cortez, L.M.C. Silva, F.B. Gonzaga, Laser induced breakdown spectroscopy, J. Braz. Chem. Soc. 18 (2007) 463–512.
[6] Q. Sun, M. Tran, B.W. Smith, J.D. Winefordner, Direct determination of P, Al, Ca, Cu, Mn, Zn, Mg and Fe in plant materials by laser-induced plasma spectroscopy, Canadian J. Anal. Sci. Spectrosc. 44 (1999) 164–170.

[7] H.H. Cho, Y.J. Kim, Y.S. Jo, K. Kitagawa, N. Araib, Y.I. Lee, Application of laser-induced breakdown spectrometry for direct determination of trace elements in starch-based flours, J. Anal. At. Spectrom. 16 (2001) 622–627.
[8] J. Kaiser, O. Samek, L. Reale, M. Liska, R. Malina, A. Ritucci, A. Poma, A. Tucci, F. Flora, A. Lai, L. Mancini, G. Tromba, F. Zanini, A. Faenov, T. Pikuz, G. Cinque, Monitoring of the heavy-metal hyperaccumulation in vegetal tissues by X-ray radiography and by femto-second laser induced breakdown spectroscopy, Microsc. Res. and Tech. 70 (2007) 147–153.
[9] O. Samek, J. Lambert, R. Hergenröder, M. Liska, J. Kaiser, K. Novotny, S. Kukhlevsky, Femtosecond laser spectrochemical analysis of plant samples, Laser Phys. Lett. 3 (2006) 21–25.
[10] S.I. Gornushkin, I.B. Gornushkin, J.M. Anzano, B.W. Smith, J.D. Winefordner, Effective normalization technique for correction of matrix effects in laser-induced breakdown spectroscopy detection of magnesium in powdered samples, Appl. Spectrosc. 56 (2002) 433–436.
[11] A. Assion, M. Wollenhaupt, L. Haag, F. Mayorov, C. Sarpe-Tudoran, M. Winter, U. Kutschera, T. Baumert, Femtosecond laser-induced-breakdown spectrometry for Ca^{2+} analysis of biological samples with high spatial resolution, Appl. Phys. B 77 (2003) 391–397.
[12] M. Sabsabi, V. Detalle, M.A. Harith, W. Tawfik, H. Imam, Comparative study of two new commercial echelle spectrometers equipped with intensified CCD for analysis of laser-induced breakdown spectroscopy, Appl. Opt. 42 (2003) 6094–6098.
[13] D. Santos Jr., F. Barbosa Jr., S.S. Souza, F.J. Krug, Cryogenic sample grinding for copper, lead and manganese determination in human teeth by slurry sampling GFAAS, J. Anal. At. Spectrom. 18 (2003) 939–945.
[14] D. Santos Jr., F. Barbosa Jr., A.C. Tomazelli, F.J. Krug, J.A. Nóbrega, M.A.Z. Arruda, Determination of Cd and Pb in food slurries by GFAAS using cryogenic grinding for sample preparation, Anal. Bioanal. Chem. 373 (2002) 183–189.
[15] E.N.V.M. Carrilho, M.H. Gonzalez, A.R.A. Nogueira, G.M. Cruz, Microwave-assisted acid decomposition of animal- and plant-derived samples for element analysis, J. Agric. Food Chem. 50 (2002) 4164–4168.
[16] J.A. Aguilera, C. Aragón, Characterization of a laser-induced plasma by spatially resolved spectroscopy of neutral atom and ion emissions. Comparison of local and spatially integrated measurements, Spectrochim. Acta Part B 59 (2004) 1861–1876.
[17] P. Stavropoulos, C. Palagas, G.N. Angelopoulos, D.N. Papamantellos, S. Couris, Calibration measurements in laser-induced breakdown spectroscopy using nanosecond and picosecond lasers, Spectrochim. Acta Part B 59 (2004) 1885–1892.
[18] B. Le Drogoff, J. Margot, M. Chaker, M. Sabsabi, O. Barthélemy, T.W. Johnston, S. Laville, F. Vidal, Y. Von Kaenel, Temporal characterization of femtosecond laser pulses induced plasma for spectrochemical analysis of aluminum alloys, Spectrochim. Acta Part B 56 (2001) 987–1002.
[19] P.A. Benedetti, G. Cristoforetti, S. Legnaioli, V. Palleschi, L. Pardini, A. Salvetti, E. Tognoni, Effect of laser pulse energies in laser induced breakdown spectroscopy in double-pulse configuration, Spectrochim. Acta Part B 60 (2005) 1392–1401.
[20] V.I. Babushok, F.C. DeLucia Jr., P.J. Dagdigian, A.W. Miziolek, Experimental and kinetic modeling study of the laser-induced breakdown spectroscopy plume from metallic lead in argon, Spectrochim. Acta Part B 60 (2005) 926–934.
[21] J.A. Aguilera, J. Bengoechea, A. Aragón, Spatial characterization of laser induced plasmas obtained in air and argon with different laser focusing distances, Spectrochim. Acta Part B 59 (2004) 461–469.
[22] B.C. Castle, K. Talabardon, B.W. Smith, J.D. Winefordner, Variables influencing the precision of laser-induced breakdown spectroscopy measurements, Appl. Spectrosc. 52 (1998) 649–657.
[23] S. Wunderli, Sampling and uncertainty — reply to the letters to the editor, Accred. Qual. Assur. 10 (2005) 255–256.
[24] NIST Atomic Spectra Database, http://physics.nist.gov/PhysRefData/ASD/lines_form.html accessed in September 2007.